

MAPPING RIPARIAN ZONES OVER LARGE REGIONS FROM HIGH SPATIAL RESOLUTION SATELLITE AND AIRBORNE IMAGERY: SPECIFICATIONS FOR OPERATIONAL MAPPING

K. Johansen^{a, b, c} and S. Phinn^{a, b}

^a Joint Remote Sensing Research Program - (k.johansen, s.phinn)@uq.edu.au

^b Centre for Remote Sensing and Spatial Information Science, School of Geography, Planning and Environmental Management, University of Queensland, Brisbane, QLD 4072, Australia

^c Centre for Remote Sensing, Dept. of Environment and Resource Management, 80 Meiers Rd, QLD 4068, Australia

KEY WORDS: Riparian Zones, High Spatial Resolution, LiDAR, Large Spatial Extents, Riparian Condition, Operational Mapping

ABSTRACT:

Riparian zones maintain water quality, support multiple geomorphic processes, contain significant biodiversity and also maintain the aesthetics of the landscape. Australian state and national government agencies responsible for managing riparian zones are planning missions for acquiring remotely sensed data covering the main streams in Victoria, New South Wales, and parts of Queensland and South Australia. The work presented in this paper provides proof-of-concept and operational specifications for using commercially available high spatial resolution satellite and airborne image datasets to map riparian condition indicators. The objectives of this paper are to: (1) assess the ability of different high spatial resolution image datasets for mapping the environmental condition of riparian zones in four distinct environments in Australia; and (2) provide specifications for capturing and analyzing the data most suited for riparian zone mapping at large spatial extents (> 1000 km of stream length). LiDAR derived digital elevation models, terrain slope, intensity, fractional cover counts and canopy height models were used to map riparian condition indicators using simple algorithms and more complex object-oriented image analysis. The results showed that LiDAR data are most suitable for mapping riparian condition indicators: water bodies; streambed width; bank-full width; riparian zone width; width of vegetation; plant projective cover; longitudinal continuity; vegetation height classes; large trees; vegetation overhang; and bank stability. Results of this work will contribute to future riparian zone mapping in Victoria, New South Wales, and parts of Queensland and South Australia.

1. INTRODUCTION AND OBJECTIVES

Riparian zones along rivers and creeks have long been identified as important elements of the landscape due to the flow of species, energy, and nutrients, and their provision of corridors creating an interface between terrestrial and aquatic ecosystems. Conventional field based approaches for assessing the environmental condition of riparian zones are site specific and cannot provide detailed and continuous spatial information for large areas, > 1000 km of streams (Johansen et al., 2007). High spatial resolution image data are required for assessment of riparian zones because of the limited width and the physical form and vegetation structural heterogeneity within riparian zones (Johansen et al., 2008a). This type of mapping has mostly been applied to riparian study areas of limited spatial extents (< 100 km of stream length) by using high spatial resolution image data. The objectives of this paper are to: (1) assess the ability of different high spatial resolution image datasets for mapping the environmental condition of riparian zones in four distinct environments in Australia; and (2) provide specifications for capturing and analyzing the data most suited for riparian zone mapping at large spatial extents (> 1000 km of stream length). This paper brings together six years of riparian mapping research based on multiple datasets from seven study sites across Australia, which has used multi-spectral satellite SPOT-5, Ikonos, and QuickBird image data and multi-spectral airborne optical (Vexcel UltraCam-D) and Light Detection and Ranging (LiDAR) data. Examples are provided from two main study areas in Central Queensland (Mimosa Creek and Dawson River) and Victoria (Werribee River, Lerderderg River, Parwan Creek, Pyrites Creek and Djerriwarrh Creek). Results from work conducted in Southeast and Central Queensland and the Northern Territory will also be presented.

2. STUDY AREAS AND DATA

The two main riparian study areas were located along Mimosa Creek and the Dawson River within a sub-tropical open woodland area in the Fitzroy Catchment, Central Queensland, and along the Werribee and Lerderderg Rivers and Pyrites, Djerriwarrh, and Parwan Creeks in the urbanized and cultivated temperate Werribee Catchment in Victoria (Table 1). Field data (28 May - 5 June 2007) were obtained around the time of image capture in the Fitzroy Catchment with a SPOT-5 image captured on 14 June 2007, two QuickBird images captured on 18 May and 11 August 2007, and LiDAR data captured on 15 July 2007. A field campaign was carried out in the Werribee Catchment between 31 March - 4 April 2008 with a SPOT-5 image captured on 20 April 2008, an Ikonos image captured on 25 April 2008, and airborne multi-spectral UltraCam-D data captured with 0.25 m pixels from 19-23 April 2008. Existing LiDAR data captured between 7 and 9 May 2005 were also used. Field data acquisition was designed to match the spatial resolution of the image data. Field measurements were obtained along transects located perpendicular to the streams of the following parameters: (1) water bodies; (2) streambed, bank-full, riparian zone, and vegetation widths; (3) plant projective cover (PPC); (4) ground cover; (5) vegetation height classes; and (6) bank stability (Johansen et al., 2008a). For calibration of the LiDAR based object-oriented mapping of streambed, bank-full and riparian zone widths, field data were collected for the bank slope and the elevation difference between the streambed and the external perimeter of the riparian zone. Where possible, existing high spatial resolution optical image data were used to locate in-situ ground control points based on invariant features visible in both the field and image data to complement GPS points to precisely overlay field and image data.

Table 1. Riparian environments, study sites, their spatial extent, and the image data used. Gray rows indicate main study areas.

Riparian environment	Study site	Spatial extent (km of stream length)	Image data used
Temperate climate, seasonal rain, hilly and flat terrain, river/creek, urbanized, cultivated and state forest	Victoria: Werribee River, Lerderderg River, Parwan Creek, Pyrites Creek, Djerriwarrh Creek	150 km	2 QuickBird images 1 Ikonos image 2 SPOT-5 images Airborne digital Ultracam-D data Airborne LiDAR data
Tropical climate, wet/dry savanna environment, flat terrain, river/creek, moderately developed for grassing and national park	Northern Territory: Daly River	21 km	2 QuickBird images 2 Landsat-5 TM images Scanned aerial photographs
	Northern Territory: South Alligator River, Barramundie Creek	30 km	1 QuickBird image 2 Landsat-5 TM images Scanned aerial photographs
Sub-tropical climate, wet/dry savanna environment, flat terrain, river/creek, moderately developed for grassing	Central Queensland: Keelbottom Creek	15 km	1 Ikonos image 1 Landsat-7 ETM+ image
	Central Queensland: Mimosa Creek, Dawson River	35 km	2 QuickBird images 1 SPOT-5 image Airborne LiDAR data Scanned aerial photographs
	Central Queensland: Isac River	10 km	Airborne HyMap data Scanned aerial photographs
Sub-tropical climate, seasonal rain, river/creek, coastal, urbanized and cultivated	Southeast Queensland: Brisbane River, Bremer River, and adjacent creeks	90 km	2 SPOT-5 images Scanned aerial photographs

3. METHODS

3.1 Mapping Riparian Zones from Optical Image Data

All satellite image datasets were atmospherically corrected to at-surface reflectance with atmospheric parameters derived from the MODIS sensor and the Australian Bureau of Meteorology. The capacity to map a number of indicators of riparian zone condition was tested for each of the datasets: water bodies; bare ground; streambed width; bank-full width; riparian zone width; width of vegetation; PPC; longitudinal continuity; large trees; large in-stream wood; vegetation overhang; and bank stability. Riparian zone width, streambed width, canopy cover, bare ground and water bodies were mapped from object-oriented image classification for all optical datasets using Definiens Professional 5 and Developer 7 (Johansen et al., 2008a; Johansen et al., in review a). Regression analysis and/or randomForest classifications were used for predicting PPC and bank stability (Johansen et al., 2008a; Johansen et al., 2008b).

Longitudinal continuity was derived from the PPC map products by defining canopy gaps as areas $> 100 \text{ m}^2$ with $< 20\%$ PPC. Mapping of large trees and in-stream wood required visual interpretation of the optical image datasets. As the use of the LiDAR data produced the best results, the remaining part of the methods section describes the approaches used to map the riparian condition indicators from the LiDAR data.

3.2 Mapping Riparian Zones from LiDAR Data

Parameters estimated from LiDAR data and used to derive information on riparian condition indicators were: digital elevation model (DEM), terrain slope, variance of terrain slope, fractional cover counts, canopy height model, and intensity (Figure 1). The output pixel size was set to minimize the pixel size and at the same time reduce the number of pixels without data, i.e. pixels without any returns, producing null values. With increased point density, a smaller pixel size could be achieved.

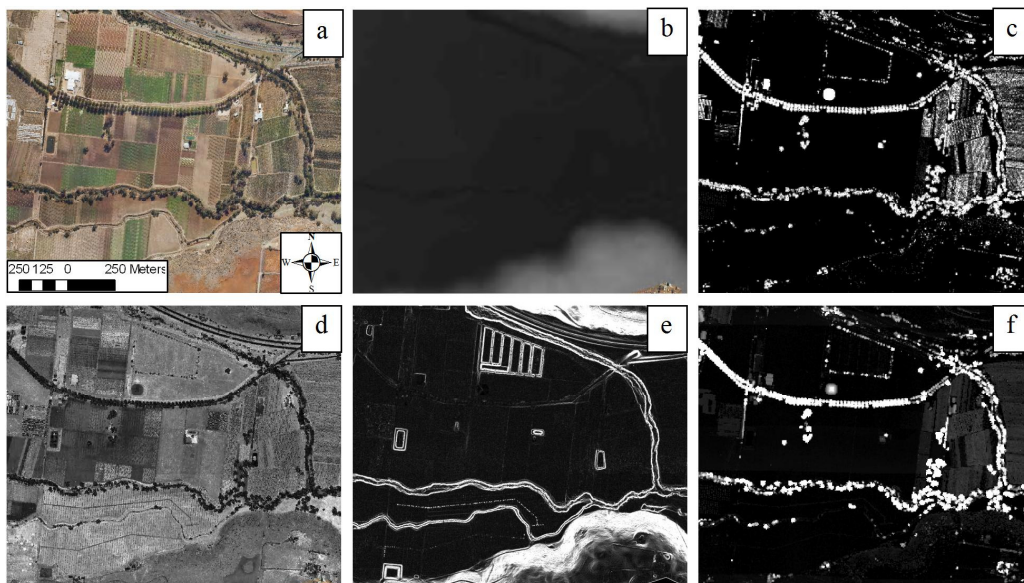


Figure 1: (a) Ultracam-D subset, and corresponding LiDAR derived raster products, including (b) DEM, (c) fractional cover counts, (d) intensity, (e) terrain slope, and (f) canopy height model. Dark areas = low values and bright areas = high values.

The DEM was produced by inverse distance weighted interpolation of returns classified as ground hits. From the DEM, raster surfaces representing terrain slope, rate of change in horizontal and vertical directions from the center pixel of a 3 x 3 moving window, and variance of the terrain slope, within a moving window of 3 x 3 pixels, were calculated. The map of fractional cover counts, defined as one minus the gap fraction probability, was calculated from the proportion of counts of first returns 2 m above ground level to correspond with the field measurements of PPC, which were derived above a height of 2 m. The height of all first returns above the ground was calculated by subtracting the ground elevation from the first return elevation. The maximum height of first returns within each pixel was also calculated. The maximum height of first returns can be considered a representation of the top of the canopy in vegetated areas (Suarez et al., 2005). The intensity band was produced by inverse distance weighted interpolation.

From the LiDAR raster products riparian condition indicators were either derived directly by using simple algorithms or object-oriented methods. Water bodies, streambed width, bank-full width, riparian zone width, and width of vegetation were mapped using image segmentation and object-oriented image classification. Water bodies were mapped from the LiDAR data using the intensity, DEM, PPC, and terrain slope bands. A local extrema algorithm was first used to find minimum values from the DEM within a searching range of 15 pixels throughout the LiDAR data extent. Only extreme minimum DEM values with an intensity < 50, a PPC value of 0, and a terrain slope < 2.5% were considered. This result was then used to grow water bodies as long the neighbouring objects had intensity mean values of less than 100 and a terrain slope < 2.5%. The streambed, defined as the area between the toes of the banks, was mapped from the DEM, terrain slope, and the variance of terrain slope using object-oriented image analysis. The segmentation process was based on the DEM and variance of terrain slope, which produced objects lining up with the gradient of the terrain and producing separate objects for the streambed, stream bank and surrounding areas because of elevation differences. The object-oriented classification of streambeds from the LiDAR data first identified the stream banks based on their steep slopes. Objects located in between steep slopes and with borders to objects with higher elevation were mapped as streambed. To map bank-full width the streambed map was expanded using a region growing algorithm to grow the streambed extent up to an elevation of 2 m above the current streambed, but limited to a distance of the original streambed by 10 m. This expanded the original streambed to include areas belonging to the bank-full width. The next step assumed that the streambed had now been expanded to include at least a small part of the lower stream bank. To reach the top of the lowest bank, the expanded streambed extent was grown further as long as the bank slope was larger than 7%, but bounded by an elevation height of 4 m above the streambed to set an upper threshold above the streambed for riparian areas surrounded by steep terrain. For mapping the extent of riparian zones, the following input bands were used for the object-oriented image analysis: PPC, canopy height model, terrain slope, DEM, and the streambed classification. The classification of the streambed was used to identify the streamside perimeter of the riparian zone. The classification of the riparian zone was then based on the distance from the streambed, the slope of the stream banks, the PPC, and the height of trees, as an abrupt change in vegetation height, density and bank slope generally occur along the external perimeter of riparian zones (Land and Water Australia, 2002). Unclassified objects within the riparian zone, i.e. riparian canopy gaps, enclosed by objects classified as streambed and

riparian zones were also classified as part of the riparian zone. The merged riparian zone polygons were then re-segmented into objects of 4 x 4 pixels, and areas, classified as riparian vegetation, with an absolute difference in elevation of more than 5 m in relation to the streambed objects, were omitted, as field data indicated that the top of banks was less than 5 m above the streambed. To map width of vegetation, the riparian zone width was merged with adjacent woody vegetation with PPC > 20%. Width of vegetation was defined as the perpendicular distance from the streambed to a non-riparian zone and non-woody vegetation pixel.

PPC was estimated from the LiDAR based fractional cover counts. Using the same procedures as Armston et al. (in press) and Johansen et al. (2008b), fractional cover counts above a height of 2 m were converted to PPC using a power function. For mapping longitudinal continuity, canopy gaps were defined as an area with less than 20% PPC and a size of at least 10 m x 10 m. The mapping of vegetation height classes was done in one step by dividing individual pixels into height categories based on the canopy height model. To avoid erroneously including agricultural fields and buildings, height categories were only obtained from those areas classified as riparian zones. Similarly, large trees were mapped as the area of the riparian canopy with trees above a height of 15 m. Vegetation overhang was mapped using the LiDAR derived streambed map and the pixel based PPC map as input bands. For areas to be classified as vegetation overhang, a minimum of 20% PPC was set as a threshold within areas classified as streambed. Bank stability was mapped from multiple regression analysis based on the relationship between field assessed bank stability and LiDAR derived PPC and terrain slope. PPC was used as tree roots from woody vegetation stabilize banks. High bank terrain slopes may indicate erosion and slumping and hence bank stability levels (Land and Water Australia, 2002).

3.3 Accuracy Assessment

The mapping accuracies of the riparian condition indicator maps were assessed using independent data from the same population wherever possible. In the cases, where only one field dataset was available, the data were randomly divided into calibration and validation data. For the maps consisting of continuous data values (e.g. PPC), R^2 values, Root Mean Square Error (RMSE), and the minimum detectable difference were calculated (Johansen et al., 2008a). The minimum detectable difference represents the smallest difference or change that would be statistically significant when comparing different samples or areas within the same or different maps. For the thematic maps, field data were used to produce error matrices and calculate associated user's, producer's, overall, and kappa accuracies.

4. RESULTS AND DISCUSSION

4.1 Comparison of Sensors and Associated Methods

The results from all study sites showed that the use of LiDAR data enabled mapping of most of the riparian condition indicators and with the highest mapping accuracies and levels of detail compared to the optical high spatial resolution image datasets. In addition to the LiDAR raster products (DEM, terrain slope, fractional cover counts, canopy height model, and intensity), the following riparian condition indicators were mapped automatically: water bodies; streambed width; bank-full width; riparian zone width; width of vegetation; PPC; longitudinal continuity; vegetation height classes; large trees; vegetation overhang; and bank condition (Figure 2).

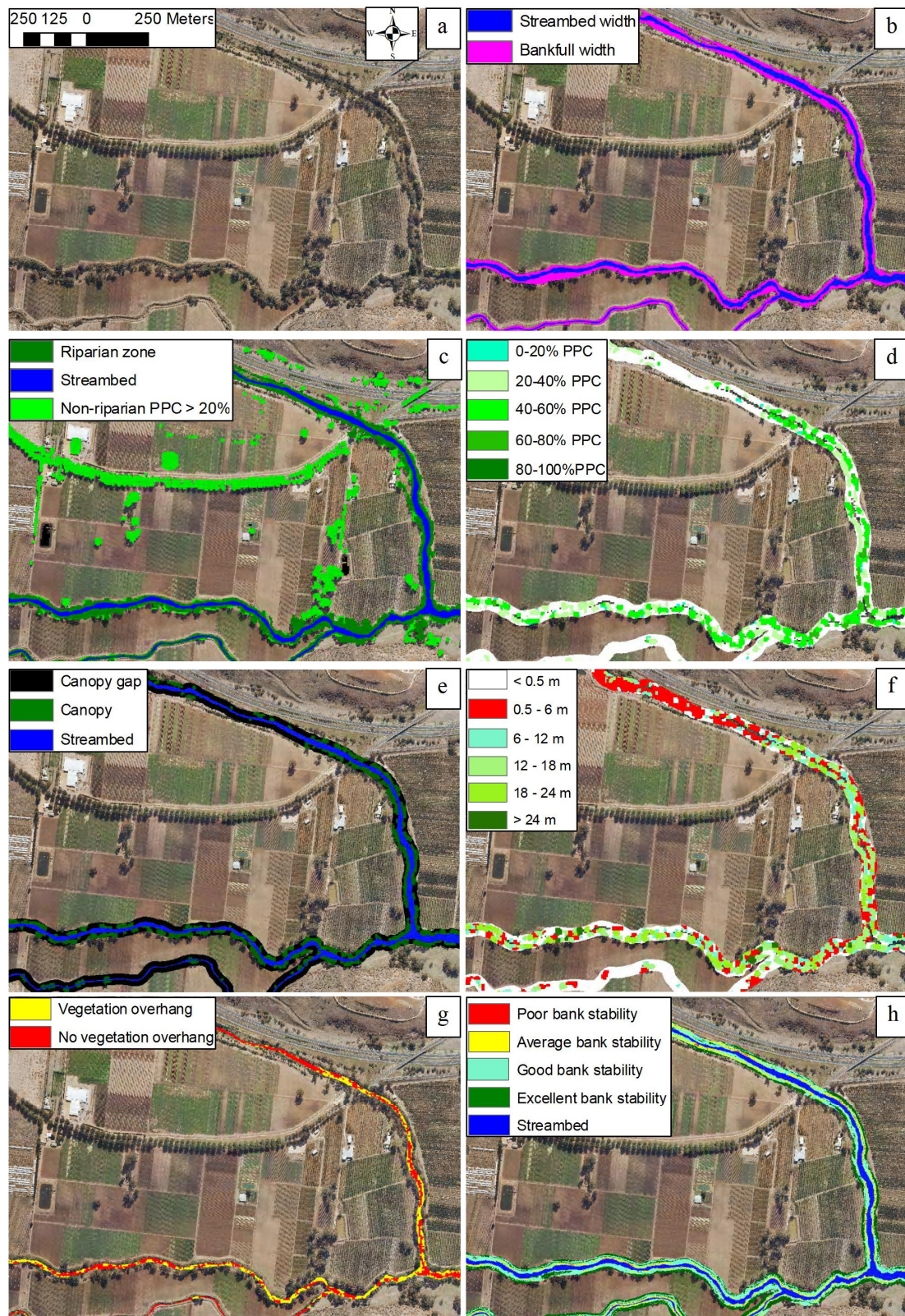


Figure 2. (a) Ultracam-D image and associated LiDAR derived maps of (b) streambed and bank-full widths, (c) riparian zone and vegetation widths, (d) PPC, (e) longitudinal continuity, (f) vegetation height classes, (g) vegetation overhang, and (h) bank stability.

Mapping accuracies of LiDAR based riparian condition indicator maps were derived from field data for the Victoria and Central Queensland study sites. Vegetation height classes and location of large trees were not validated because of the high vertical accuracy of the point clouds (< 0.20 m). Field measurements of streambed (RMSE = 3.3 m, $n = 17$), bank-full

(RMSE = 6.1 m, $n = 17$) and riparian zone widths (RMSE = 7.0 m, $n = 17$) were compared directly with the corresponding locations within the maps. PPC was validated against an independent field dataset and had a RMSE of 12% PPC ($n = 110$). The mapping accuracies of vegetation overhang and longitudinal continuity were direct derivatives of the streambed

and PPC maps. Compared against field data, LiDAR derived bank stability based on the terrain slope and PPC maps was mapped with an $R^2 = 0.40$ using multiple regression analysis. In all cases, the LiDAR derived riparian condition indicator maps were more accurate than those produced from the high spatial resolution optical datasets. The airborne Ultracam-D image classification of water bodies produced similar high user's and producer's accuracies to those from the LiDAR data classification, but was unable to detect water bodies obstructed by canopy cover, which in particular was a problem for narrow streams. Overall, the LiDAR data required less intensive processing than the optical datasets, because of the inherent high precision and provision of 3-dimensional information and the smaller number of bands needed for the riparian condition indicator mapping. The Ultracam-D image data with 0.25 m pixels required very extensive and time-consuming processing, e.g. 18 days of constant processing to produce the PPC map for 195 km² using the randomForest algorithm.

The Ultracam-D, Ikonos, and QuickBird image data could be used for mapping the following indicators for most study sites: water bodies; bare ground; PPC; longitudinal continuity; width of vegetation; and riparian zone width. However, riparian zone width was overestimated in areas with topographically complex terrain (e.g. RMSE = 38 m, n = 12) and with adjacent dense sub-tropical and tropical woodland and temperate state forests (e.g. RMSE = 45 m, n = 15). In contrast, LiDAR data could be used successfully in these areas using bank slope information and thresholds of the difference in elevation between the streambed and the external perimeter of riparian zones. The Ultracam-D image data were also found useful for visual calibration and validation of the LiDAR derived indicator maps of water bodies, streambed width, bank-full width, and riparian zone width. Large trees defined by their tree crown diameter (> 15 m in any one direction) and large in-stream wood could in most cases be visually delineated from the Ultracam-D image data (0.25 m pixels) although tree crowns in densely vegetated areas could not be separated and large in-stream wood could only be identified in open areas. Automatic delineation of tree crowns was not possible, as the complex and densely vegetated riparian zone canopy structure did not fulfill the requirements of existing algorithms relying on a bright apex and shaded areas surrounding the crown perimeter (Johansen et al., 2006).

One major limitation of the optical image datasets for riparian zone mapping was the requirement of a very accurate image classification for mapping water bodies, bare ground, PPC and longitudinal continuity. Water bodies were difficult to map accurately because of obstruction and shadows from tree crowns along the stream edge. The algorithms used to map PPC and the longitudinal continuity derivative cannot distinguish between woody and non-woody vegetation such as agricultural and grass cover. Therefore, accurate image classification of woody and non-woody vegetation is required to produce a mask. High spatial resolution image data are generally difficult to accurately classify into land-cover classes because of the large reflectance variation of individual features at these spatial resolutions. Object-oriented image classification is the only suitable means to achieve accurate image classification results, but currently no suitable rule sets are available for multi-site use, i.e. riparian zones occurring in for example urban, cultivated, woodland, rangeland, and forest environments.

The spatial dimensions of the river-riparian zone system affected the accuracies of the mapping results of the optical image datasets, as the mapping accuracies relied on the interaction of spatial resolution with the spatial scale of features

in the riparian environment being imaged. For example, the spatial resolution of the QuickBird image data was more suitable for mapping large river-riparian zone systems (e.g. the Daly River, river width > 40 m and riparian zone width 50 – 100 m) than those in the Werribee Catchment (e.g. the Werribee River, river width < 20 m and riparian zone width 10 – 30 m). The distinct vegetation zonation and the large sections of bank slumping along the Daly River enabled more accurate mapping with the QuickBird image data of e.g. PPC and bank stability than along the Werribee River. The SPOT-5 image data were not suitable for mapping riparian condition indicators, because of the limited spatial resolution in relation to the streams and associated riparian zones mapped.

In the temperate study site in Victoria, it was found important to map riparian zones in the leaf-on season, as the amount of canopy cover will significantly affect a large number of riparian condition indicators. In riparian environments dominated by evergreen and semi-deciduous tree species, it was found less important to capture LiDAR data in any particular season. However, optical image data should be captured in the dry season to reduce effects from understorey vegetation and to accurately map riparian zone width (Johansen et al., 2008a).

4.2 Specifications for LiDAR Data Acquisition and Analysis

LiDAR sensors designed for corridor mapping, such as the Toposys Harrier 56/G3 Riegl LMS-Q560, were considered most appropriate for cost-effectively and consistently mapping riparian condition indicators for areas > 1000 km of stream length. These systems also enable capture of coincident very high spatial resolution image data on an opportunistic basis when weather conditions permits optical data capture. A low-cost coincident optical image dataset would be very suitable for calibration and validation of LiDAR derived riparian condition indicator maps and for visual interpretation of large in-stream wood. The use of LiDAR data also proved more cost-effective at these spatial scales compared to satellite and airborne optical image datasets (Johansen et al., in review b). The LiDAR data were found more appropriate for acquisition and analysis than the optical image datasets because of consistent scan angles, ability to capture data in cloudy conditions, and capacity for mapping automation. The acquisition of airborne LiDAR data is possible over a shorter period of time than that for optical image datasets, as LiDAR data acquisition is less weather dependent and can be captured day and night if required. LiDAR specifications deemed most suitable for riparian mapping applications based on the experiences gained for the study sites in Victoria and Central Queensland and the literature (Goodwin et al., 2006; Armston et al., in press) are presented in Table 2.

Table 2: Some suggested LiDAR data acquisition specifications for riparian mapping applications.

Parameters	Value
Scan angle	< 15 degrees
Maximum scan angle	45 degrees
LiDAR overlap between runs	30%
Point spacing	0.50 m along/across track
Point density	4 points/m
Spot footprint	0.30 m
Sensor settings to be reported	Maximum scan angle; pulse rate; scan frequency; X, Y, and Z uncertainty
Format	Las 1.1 to store geo-referenced information without any approximations
Return intensity	Radiometrically calibrated
Point cloud classification	Into ground and non-ground

As the intrinsic attributes of riparian features being mapped will vary depending on location and the feature being assessed, the extrinsic specifications of the LiDAR data acquisition will need to suit a wide range of requirements. The canopy gap size distribution affects the dynamic range of estimates of cover as the LiDAR beam is “blind” to gaps smaller than its cross-sectional area. Previous work over a range of vegetation types has indicated that an average point spacing of < 1 m and a maximum beam cross-sectional diameter < 30 cm will provide good mapping precision up to approximately 90% foliage cover (Armston et al., in press). The scan angle should be minimized (at least < 15°) to limit the effects of leaf angle distribution and ground slope on spatial variation in cover profile estimates in order to avoid more advanced modeling (Goodwin et al., 2006). To obtain information on riparian forest structure at a spatial scale suitable for dense vegetation as well as smaller streams with narrow riparian zones (< 20 m wide), the point density should be at least 4 points / m² (> 0.5 m point spacing). With a set laser beam divergence at 0.5 mrad, a flying height of ≤ 600 m is required to achieve a footprint size of ≤ 30 cm diameter. It is recommended that an area of at least 100 m beyond the external perimeter of the riparian zone on each side of the stream is covered. A total swath width of 500 m would be sufficient for the majority of streams and associated riparian zones in Australia. To achieve a swath width of 500 m with a scan angle < 15° and a footprint size ≤ 30 cm diameter, two parallel strips with 30% overlap will need to be flown. Scan frequency and platform speed are to be determined to optimize point density, the altitude of the platform, the maximum scan angle, and the beam divergence, which, in combination with altitude, dictates the ground footprint size (Goodwin et al., 2006). Metadata are required to provide detailed and complete documentation of the acquisition as well as independent accuracy assessment using field data obtained at the time of LiDAR data acquisition. It is also important that specific processing documentation is developed to the extent, where the processing routines can be precisely repeated. This is important for successful future monitoring of streams and riparian zones.

5. CONCLUSIONS AND FUTURE WORK

Our findings show that high spatial resolution passive and active image data can be used for mapping riparian zone properties over large spatial extents. LiDAR data, if captured with suitable specifications, are more appropriate and cost-effective than SPOT-5, QuickBird, and Ikonos satellite image data and airborne multi-spectral UltraCam-D image data for mapping riparian condition indicators. Although the use of the UltraCam-D dataset enabled mapping of more riparian condition indicators than the other assessed optical image datasets, the Ultracam-D image data were not suited for mapping riparian condition over large spatial extents from a cost-benefit perspective due to the large file size, requiring extensive and very time-consuming data processing for automated procedures. LiDAR data could be used to accurately map the largest number of riparian condition indicators: water bodies; streambed width; bank-full width; riparian zone width; width of vegetation; PPC; longitudinal continuity; vegetation height classes; large trees; vegetation overhang; and bank condition. Overall, the LiDAR data required less intensive processing than the optical datasets. The LiDAR data were found most appropriate for acquisition for large regions because of consistent scan angles, ability to capture data over shorter time frames, and capacity for mapping automation. Future work will focus on mapping applications at the state level in Australia for > 100,000 km of stream length.

REFERENCES

- Armston, J., Denham, R., Danaher, T., Scarth, P., and Moffiet, T., in press. Prediction and validation of foliage projective cover from Landsat-5 TM and Landsat-7 ETM+ imagery for Queensland, Australia. *Journal of Applied Remote Sensing*.
- Goodwin, N.R., Coops, N.C., and Culvenor, D.S., 2006. Assessment of forest structure with airborne LiDAR and the effects of platform altitude. *Remote Sensing of Environment*, 103(2), pp. 140-152.
- Johansen, K., and Phinn, S., 2006. Mapping structural parameters and species composition of riparian vegetation using IKONOS and Landsat ETM+ data in Australian tropical savannahs, *Photogrammetric Engineering and Remote Sensing*, 72(1), pp. 71-80.
- Johansen, K., Dixon, I., Douglas, M., Phinn, S., and Lowry, J., 2007. Comparison of image and rapid field assessments of riparian zone condition in Australian tropical savannahs. *Forest Ecology and Management*, 240, pp. 42-60.
- Johansen, K., Phinn, S., Lowry, J., and Douglas, M., 2008a. Quantifying indicators of riparian condition in Australian tropical savannahs: integrating high spatial resolution imagery and field survey data. *International Journal of Remote Sensing*, 29(3), pp. 7003-7028.
- Johansen, K., Clark, A., Denham, D., Armston, J., Phinn, S., and Witte, C., 2008b. Mapping plant projective cover in riparian zones: integration of field and high spatial resolution QuickBird, SPOT-5 and LiDAR data. In *Proceedings of the Australasian Remote Sensing and Photogrammetry Conference*, Darwin, Australia.
- Johansen, K., Arroyo, L.A., Armston, J., Phinn, S., and Witte, C., in review a. Mapping riparian condition indicators in a sub-tropical savanna environment from discrete return LiDAR data using object-oriented image analysis. *Trees: Structure and Function*.
- Johansen, K., Phinn, S., and Witte, C., in review b. Multi-scale mapping of riparian zone attributes using LiDAR, QuickBird and SPOT-5 imagery in Australian sub-tropical savannahs: assessing accuracy and costs. *Forest Ecology and Management*.
- Land and Water Australia (2002). *River landscapes; fact sheet*. Land and Water Australia, Canberra, Australia.
- Suarez, J.C., Ontiveros, C., Smith, S., and Snape, S., 2005. Use of airborne LiDAR and aerial photography in the estimation of individual tree heights in forestry. *Computers and Geosciences*, 31, pp. 253-262.

ACKNOWLEDGEMENTS

Lara Arroyo, Michael Hewson, and Eric Ashcroft from the Centre for Remote Sensing and Spatial Information Science at University of Queensland, Australia, and Andrew Clark, John Armston, Peter Scarth, Christian Witte, Robert Denham, and Sam Gillingham from the Remote Sensing Centre at QLD Department of Environment and Resource Management, Australia and Paul Wilson, Sam Marwood and John White from the Department of Sustainability and Environment, Victoria provided significant help with fieldwork and image processing.